ISES International Solar Energy Society

Conference Proceedings

EuroSun 2014

Aix-les-Bains (France), 16 - 19 September 2014

Hydration / dehydration cycles of salt hydrates – studied with NMR–

P.A.J. Donkers[1,2], L. Pel[2], O.C.G. Adan[2,3]

[1]Materials innovation institute M2i, Delft (Netherlands)

[2] Eindhoven University of Technology, Eindhoven (Netherlands)

[3] TNO, Delft (Netherlands)

Abstract

A heat buffer is the missing link for introduction of renewable energy on a large scale. Salt hydrates are a promising technique to fulfill this task. In this study, we focused on reversibility of sulfate hydrates dehydration/hydration cycles. Different hydrates are studied with TGA and Nuclear Magnetic Resonance (NMR). Two hydrates were selected to perform cyclic experiments: $CuSO_4$ and $MgSO_4$. Several heating and cooling cycles are followed with help of NMR. Pore water was only observed during the first dehydration cycle.

Keywords: Thermochemical heat storage, NMR, sulfates.

1. Introduction

Systems that buffer heat are needed to match the demand and supply of renewable energy. A promising storage system is based on hydration and dehydration of salts. A major advantage is the long time storage and the reversibility of the reaction. The heat density is such systems can be in the order of 2 GJ/m^3. In current research is found that the reversibility is not always reached (Ervin, 1977), e.g. the capacity of water to lose and absorb drops for $Mg(OH)_2$ from 95% to 60-70% within 40 cycles. In addition, hydration/dehydration rates can decrease if more cycles are applied, e.g. 2 times slower for $Ca(OH)_2$.

For the development of a storage system with high stability, additional knowledge is needed about the dehydration and hydration process. Especially understanding of the absorbing and desorbing process of water on the crystal structure is important. In equilibrium situations the positions of the water molecules in a crystal and the structure can be analyzed with several techniques, like X-RAY, Raman and IR. In non-equilibrium experiments techniques are used like Thermo Gravical Analysis (TGA) and Dynamic Scanning Calorimetry (DSC).

A technique which can measure the mobility of water in combination with the amount of water will improve the knowledge on the dehydration and hydration processes of salts. In this project, we use Nuclear Magnetic Resonance (NMR) to study how water absorbs/desorbs during a dehydration/hydration cycle.

2. Experimental setup

In this study NMR is used to measure non-destructively water in a material. The signal of water attenuates in a NMR experiment according to:

$$S(t) = \rho\left(1 - \exp\left(\frac{t_r}{T_1}\right)\right)\exp\left(-\frac{t}{T_2}\right) \qquad \text{(eq.1)}$$

Here ρ is the proton density, t_r is the repetition time of the measurement sequence, T_2 the transversal relaxation time and T_1 the longitudinal relaxation time. According to this equation it is possible to link the signal intensity of the NMR to the amount of water. To avoid the influence of the longitudinal relaxation time, the repetition time of the experiments is chosen as $t_r > 3\ T_1$. Secondly, the influence of T_2 is tried to

Selection and/or peer review under responsibility of EuroSun2014 Scientific Committee
doi:10.18086/eurosun.2014.10.10 Available at http://proceedings.ises.org

minimize, so the measurement time (t) should be chosen as close as possible to zero. Measuring at $t = 0$ is from practical point of view not possible and for that reason the entire signal decay was recorded using the CPMG pulse sequence (Meiboom and Gill, 1958). During the CPMG pulse sequence a static magnetic field gradient of 270 mT m^{-1} is applied. This small gradient adjusts the echoes of the CPMG pulse train in our recording window. The time between two successive echoes within the pulse sequence was 60 µs, the repetition time of the sequence was 24 s, 1024 till 4096 echoes were recorded and an accumulation of 4 scans was performed. A fast Laplace inversion transformation (FLI), Song et al., 2002, was used to analyze the T_2 decay curves and calculate the proton density.

With help of the T_2 measured with a CPMG measurement it is possible to distinguish mobile and immobile water molecules. In general the T_2 can be related to the mobility of the proton, whereby the T_2 increases with increasing mobility. Two groups of transversal relaxation times (T_2) can be observed in hydrates. The first group has T_2 values between 10 to 400 µs, which will be referred to as lattice water and the second group has T_2 values between 1 and 1000 ms, which is called pore water. We define lattice water as water which is connected to the salt structure and is immobile. All other water in the grains will be referred to as pore water.

For measuring hydrates during dehydration/hydration, we used a home-build RF-coil which resonances at 200MHz (see Figure 1). With this coil it is possible to perform quantitative analysis of the NMR signal, because of the use of a Faraday coil. The temperature can be controlled of the range of 20-150°C within ±1 K. Samples with a size of 10 mm height and 6 mm diameter are place in a glass cylinder. The glass cylinder is open from two sides and with help of air flow the RH is controlled. The air flow is kept constant at 0.2 L/min. All experiments were performed at atmospheric pressure. The advantage of this setup is that the air can blown through the sample, while which most other techniques this is impossible.

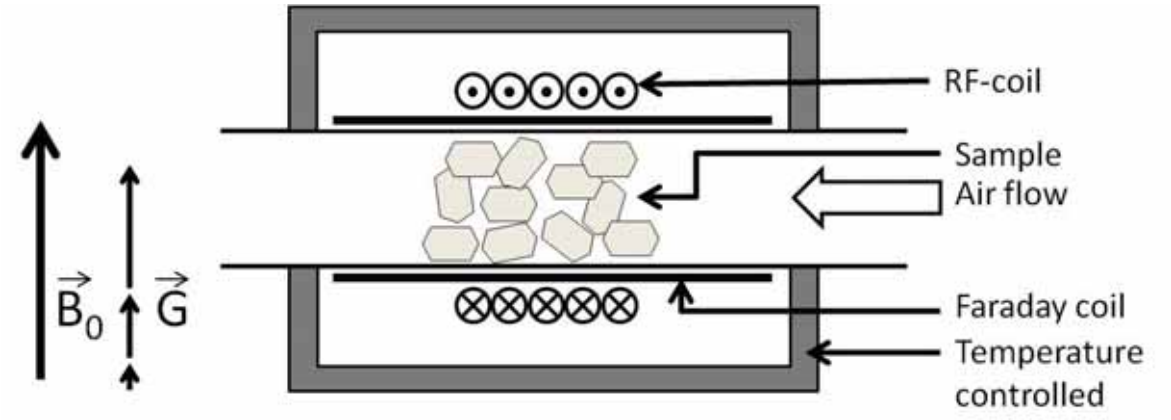

Figure 1: The NMR setup used during dehydration experiments. The sample can be conditioned by vapor pressure and temperature.

3. Single dehydration measurements

The first approach is to study sulfate salts with the metals Mg^{2+}, Co^{2+}, Cu^{2+} and Zn^{2+}. They are equilibrated at a constant relative humidity with help of saturated salt solutions. Depending on the RH, these complexes can form all a stable hepta- and hexahydrate at 25°C. The exception is Cu^{2+}, which can maximally form a pentahydrate at 25°C.

3.1 TGA experiments

Initially, the salts were measured with TGA (TG50 of Mettler Toledo), with a heating rate of 0.61 K/min. Dry nitrogen was blown over the samples. The samples had sizes of approximately 10 mg and were placed in a standard alumina pan of 40µl with a hole of 1 mm in the lid to permit water vapor to escape.

The results are shown in figure 2. As can be seen after heating till 150°C, only one water molecule is left over. This last water molecule is released between 200 and 300°C.

With help of phase diagrams the TGA curves are analysed, for example for $CoSO_4.7H_2O$. In Figure 3 the phase diagram of $CoSO_4$-H_2O is given in temperature and vapor pressure, which is composed of different literature sources (Washburn, 2003; Kohler and Zaske, 1964; Broers and van Welie, 1965). Each line or dot

represents an equilibrium RH-T of two phases, what can be two hydrates or a hydrate and its saturated solution. These three sources are not in agreement with each other, for example the phase equilibrium between $CoSO_4.7H_2O$-solution was measured by two sources, but different values are reported. Additionally the paper of Kohler and Zaske, 1964 is discussed by Broers and van Welie, 1966, wherein they doubt the accuracy of these measurements.

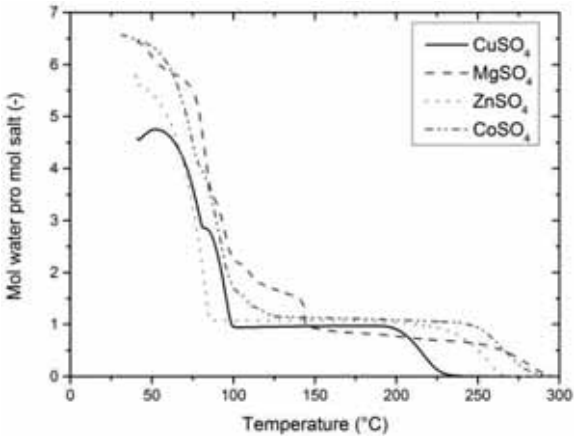

Figure 2: The mol water pro mol salt as determined by TGA for a heating rate of 0.61 K/min. The samples had an initial weight of 13±2 mg.

$CoSO_4$ starts to loose water molecules in the TGA experiment at 60°C. It has a small discontinuity by 4 water molecules water pro mol $CoSO_4$ at 80°C, while it dehydrates till it's monohydrate at 120°C. These temperatures and loadings are not in agreement with the phase diagram of figure 3. Firstly, according to the phase diagram the first transition is expected at 48±2°C. Secondly, a stable phase of $CoSO_4.4H_2O$ is not measured in the literature. The difference can be a result of the non-equilibrium situation of the TGA experiment, while the phase diagram is measured in equilibrium situations. Additional information about the composition of the sample is needed to understand the difference between the phase diagram and the TGA experiment.

A more detailed discussion of the TGA curves of the other three salts will be given in combination with the NMR experiments in section 3.2.

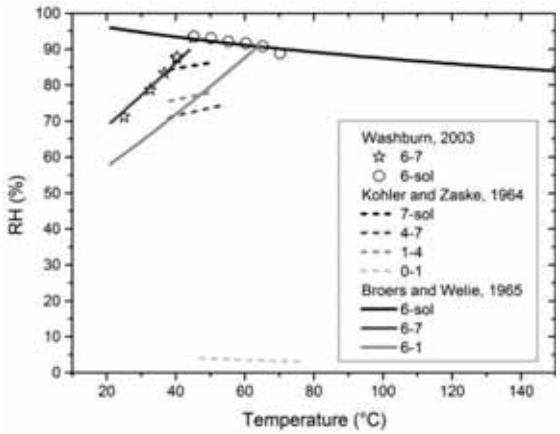

Figure 3: The phase diagram of $CoSO_4$-H_2O in the temperature range of 25-150°C existing of data of Washburn, 2003, Kohler and Zaske, 1964 and Broers and Welie, 1965.

3.2 NMR experiments

In Figure 4A the NMR results are plotted of the dehydration of $CoSO_4.7H_2O$. The total water signal intensity measured with NMR can be compared with the TGA experiments. This signal intensity can be divided in two groups of water, i.e. lattice and pore water, with help of relaxation analysis as explained in section 2.

Comparing the results of the TGA in figure 2 and total water component of the NMR measurement, the experiments are in good agreement with each other. The shift to higher temperatures in case of the NMR experiments was expected because of larger samples used (Crowther and Coutts, 1924). Comparing the NMR measurement with the phase diagram, an abrupt decrease of lattice water would be expected at 48°C as

a result of the phase transition of the hepta-hydrate to the hexa-hydrate. If the vaporized lattice water cannot diffuse out of the grain, the vapor will condensate and pore water will be measured with NMR. According to the NMR measurements almost all water vapor condensates and partially dissolves the grains. After condensation the grains start to release its pore water gradually. The lattice water stabilizes till it starts to decrease around 80°C as well and is finished at 130°C. A second sharp transition like at 50°C is not observed at higher temperatures by the NMR measurements, this can be a result of the observed pore water. With help of the solubility of $CoSO_4$ and the NMR results, the loading of the lattice water in $CoSO_4$ is calculate which was between 50-80°C 5 water molecules pro $CoSO_4$. This implies a 4:1 mixture of $CoSO_4.6H_2O$ and $CoSO_4.1H_2O$ according to the known hydrates of $CoSO_4$. Our hypothesis is that the saturated $CoSO_4$ solution will decrease the dehydration rate and results in a continuously dehydration instead of the fast transition as at 50°C.

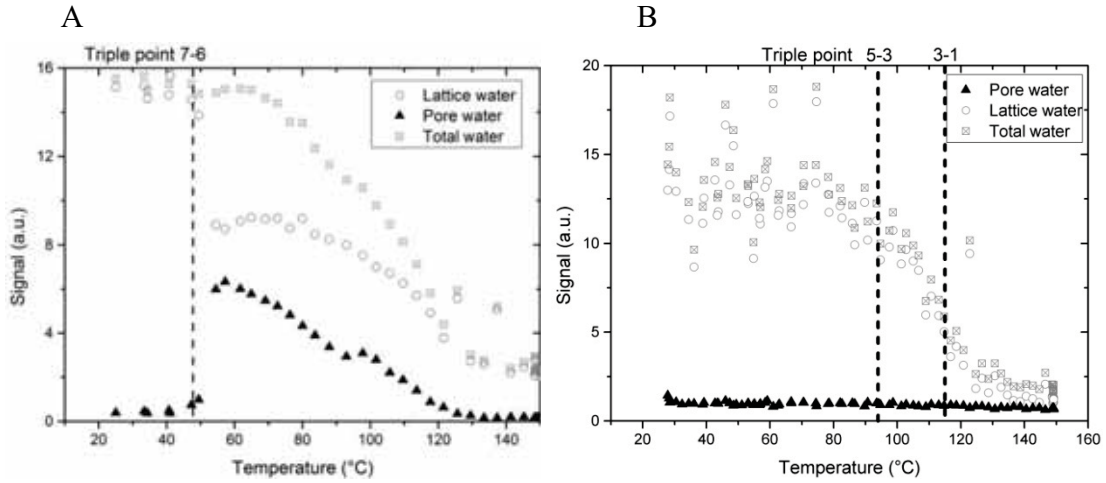

Figure 4: The dehydration of $CoSO_4.7H_2O$ in figure 4A and $CuSO_4.5H_2O$ in Figure 4B with 0.61 K/min with NMR. The signal intensity plotted against temperature; hereby the total water amount is divided in two types of water: lattice and pore water. The dashed lines indicate the temperatures of the known triple points of this salt water system.

In Figure 4B the results of the dehydration of $CuSO_4$ is shown, whereby the total water signal is again divided in lattice and pore water. In the figure the two triple points of the $CuSO_4$ hydrates are indicated, where $CuSO_4$ should dehydrate to the other phase according to the phase diagram. For $CuSO_4.5H_2O$ the total signal intensity initially decreases around 80°C and is stable at a temperature of 120°C. During this measurement no pore water is observed, and no abrupt changes in lattice water. The results of the TGA measurement of figure 2 and the NMR measurements are again in good agreement with each other. No stepwise dehydration is observed during the NMR experiment from five to three and further to one water molecule pro $CuSO_4$ molecule. This is a result of the used sample size, what was also observed by Hume and Colvin, 1931. The results of both TGA and NMR are in agreement with the phase diagram of $CuSO_4$-H_2O.

In figure 5A, the results of the NMR experiments of $MgSO_4$ are shown. The total signal is again divided in the same way as in the previous experiments into pore and lattice water. The TGA and total signal intensity match with each other. Focusing on the lattice and pore water, a similar process is observed as in case of $CoSO_4.7H_2O$. Around 50°C a strong increase of pore water is observed by crossing the triple point of $MgSO_4.7H_2O$, $MgSO_4.6H_2O$ and solution. In the temperature range of 50-90°C, the lattice water results in an average loading of 5 molecules of water on $MgSO_4$. The second increase of pore water at 90°C does not match a triple point in the used phase diagram, an explanation for this is lacking. This might be explained by pore water effects.

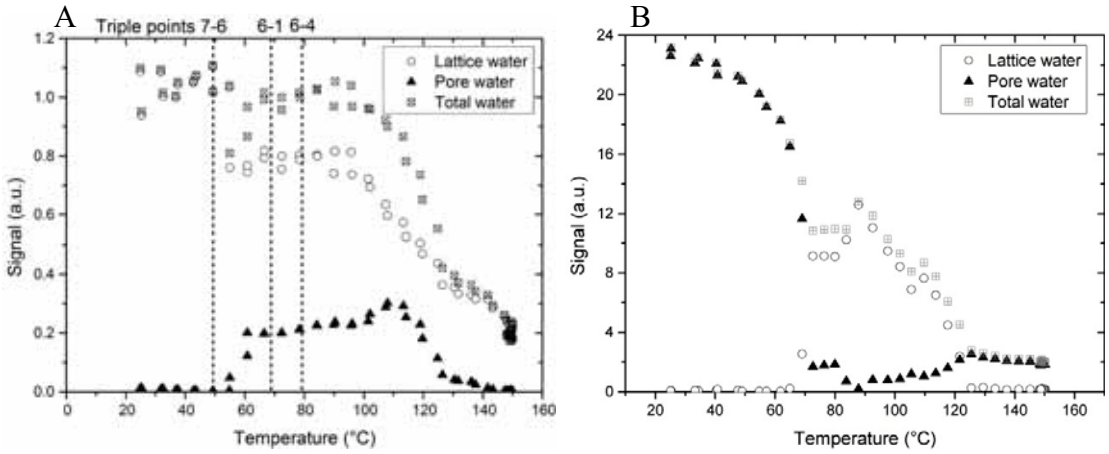

Figure 5: The dehydration of$MgSO_4.7H_2O$ in figure 5A and $ZnSO_4.6H_2O$ in Figure 5B with 0.61 K/min with NMR. The signal intensity plotted against temperature; hereby the total water amount is divided in two types of water: lattice and pore water. The dashed lines indicate the temperatures of the known triple points of this salt water system (Steiger et al., 2011).

In Figure 5B the dehydration of $ZnSO_4.6H_2O$ is shown. The total water signal drops from the start of the experiment, till 120°C. Compared to the TGA experiment, the finial signal intensity is lower as expected at 150°C. This is a result of the dissolving of the grains, what was observed after opening the sample holder. By analyzing the pore and lattice water content, the salt shows at 70°C an almost complete dissolving of the crystal. The position of the transition hexa to monohydrate is not well defined in literature, so we cannot compare it with the transition point of these two hydrates. From 90°C on, $ZnSO_4$ start to recrystallize and at 120°C the salt reached its hydrated state $ZnSO_4.H_2O$.

Based on these experiments, we decided to study $MgSO_4$ and $CuSO_4$ in the cycling experiments.

4. Cycling experiments

During cycling experiments the temperature was raised during dehydration from 25 °C to 150 °C by 0.61 °C/min. After reaching 150°C, the temperature is decreased till 25-30 °C in 1 hour (no active cooling present). During rehydration for 15-24 hours air is blown through the sample with a RH of 50-70% in case of $CuSO_4$ and 80% in case of $MgSO_4$.

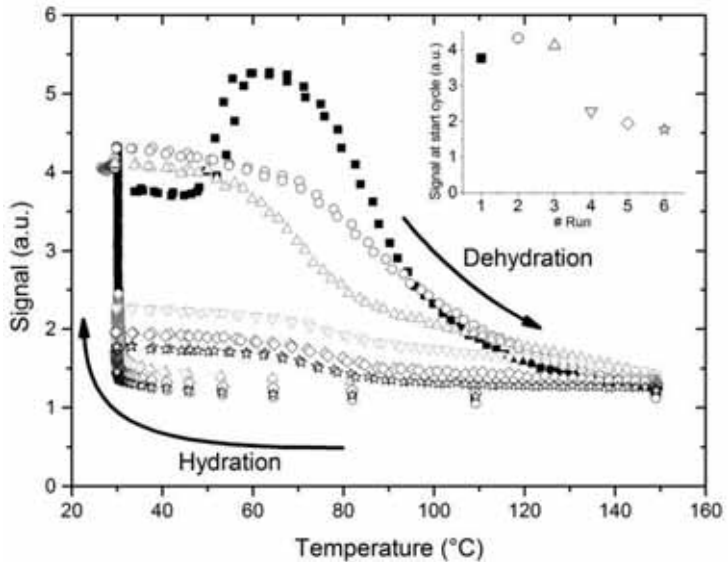

Figure 6: The result of six runs of dehydration-hydration cycles of $MgSO_4.7H_2O$; hereby dehydration is performed with 0.61 K/min at 0% RH and the hydration at 30 °C at with an airflow of 22 °C and 80% RH. The signal intensity plotted against the temperature for the different runs. In the inset the signal intensity at the start of a cycle is plotted against the number of the run.

4.1 $MgSO_4$

In Figure 6, the NMR signal intensity is plotted versus the temperature of the sample during the cyclic hydration/dehydration of $MgSO_4$. In the inset the signal intensity is plotted of the crystal before dehydration of each run. Initially the water content is 6.5 water molecules pro $MgSO_4$ molecule at 30 °C. During the first run the signal intensity increases around 50 °C as result of the production of pore water, like we observed by the dehydration experiment in figure 5A. At the beginning of the second run, the water content is higher than initially. This can be contributed to a rehydration till 7 water molecules pro $MgSO_4$.

The other runs show a decrease of hydration level at the end of the hydration run, see inset. No pore water is observed during these runs, so the crystals dehydrate without crossing the deliquescence line. This means that the vapor transport rate is larger than by fresh crystals. That the structure of the crystals is affected by dehydration has been observed before and is described by a psuedomorph structure (Mutin and Watelle, 1979**)**. In this model the grain is divided in a compact assembly of well defined microcrystals whereby the grain keeps its outer shape.

In figure 7 a schematic representation is given of the dehydration-hydration process of $MgSO_4$ with the crystals during the different hydration/dehydration runs. Our hypothesis is that the space in-between the microcrystals create pathways for releasing of the water molecules out of the crystal grains. During the first dehydration step, the crystal forms a pseudomorphic structure with cracks. These cracks will be used as water pathways during rehydration. First the outer shell of the grains absorbs water and the new formed hydrates will narrow the pathways of the water vapor to the inner part of the grains. During dehydration the new formed hydrates will form small microcrystals which can rehydrate quicker. This will result that the pathways will be blocked faster, what will decrease the total rehydration rate. So the inner part can still rehydrate, but the water supply is blocked by a layer of freshly rehydrated $MgSO_4.7H_2O$. During every run the easily accessible layer will become smaller until only the outer layer reacts on the change in RH.

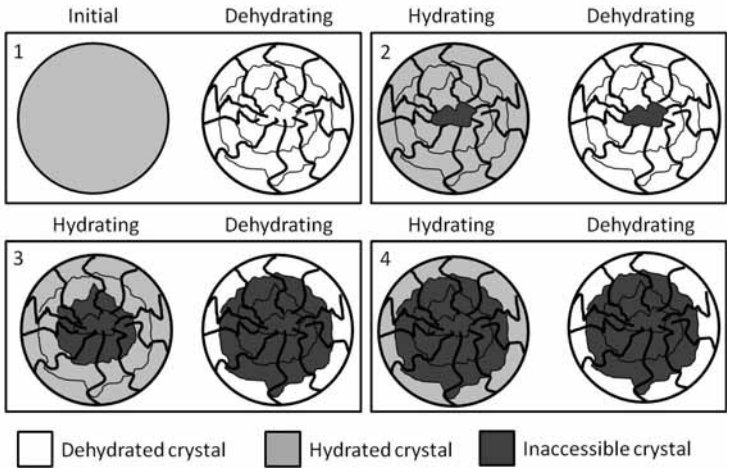

Figure 7: A schematic representation of the dehydration-hydration process of $MgSO_4$ where the grain is cracked during the first dehydration run. In the next runs every time a smaller area of the crystal is accessible for the water vapor applied during hydration, because more cracks will be blocked during rehydration.

The inset in figure 6 shows that the initial signal intensity decreases abrupt between the third and the fourth cycle. This can be a result of different hydrate loadings or a smaller ratio of active material. For that reason, in Figure 8 the water loss ratio is plotted against temperature. The water loss is normalized from maximum and minimum signal intensity during each run. Comparing the different curves, the shapes of each single curve fits with the average curve within 10 °C. Therefore, we expect that the formed hydrates have the same loading every run, only the amount of active hydrates decreases. This strengthens our hypothesis about the smaller volume of active grain during increasing number of hydration/dehydration cycle.

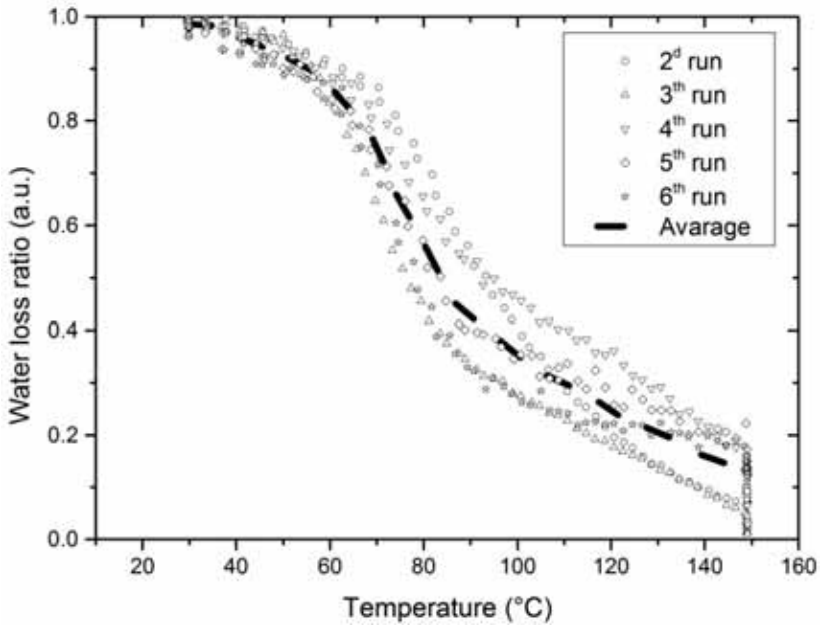

Figure 8: The signal scaled from 0 to 1 for each run plotted against temperature. We see that every time the dehydration curve has a similar shape, what indicates that the 'active' hydrates rehydrate till the same hydrate state during rehydration.

4.2 $CuSO_4$

In figure 9 the results are plotted of a rehydration experiment with $CuSO_4$. The signal intensity of the NMR is plotted against the time, where on the right vertical axes the temperature and RH are plotted. The inset shows the signal intensity before dehydration for each run. As can been seen, the signal intensity of the sample does not reach the initial signal intensity during the first 3 runs where the applied RH 50% is. This is a result of the short cycling time in combination with the small difference between the equilibrium RH and the applied RH. By increasing the relative humidity to 70% in the other 4 cycles the dehydration was still incomplete. The measured signal intensities shows that during the first 3 rehydration runs the average hydration state was almost three, while the hydration state for the last 3 rehydration cycles is 4.3.

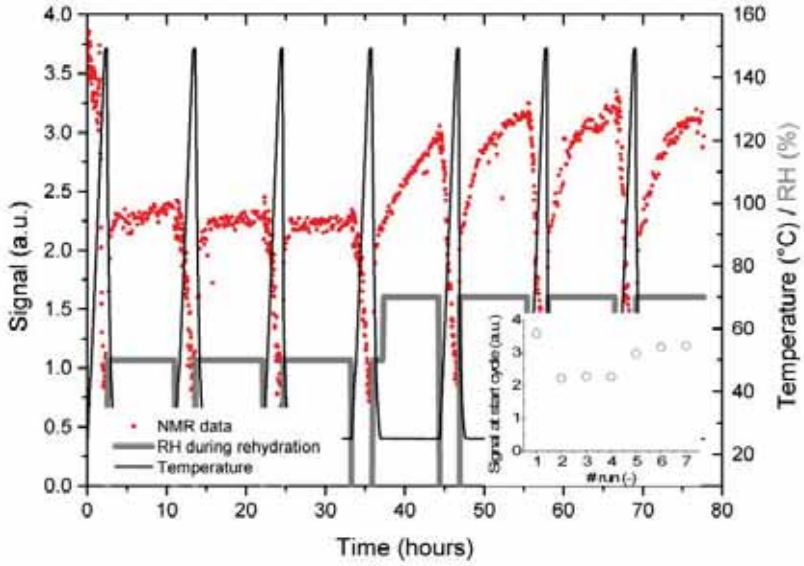

Figure 9: Six runs of dehydration-hydration cycles of $CuSO_4.5H_2O$. The dehydration is performed with 0.61 K/min at 0% RH and the hydration at 25°C. The inset shows the signal intensity at the start of the signal for each run.

Figure 10 shows the signal intensity normalized on the initial and final signal intensities of the different dehydration cycles plotted against temperature during dehydration. It shows that the grains release their water differently the first run from the other six runs. It releases its water at a much higher temperature of

120 °C compared to 60 °C in other runs, measured at the bending point in the dehydration curve. This is again a result of the pseudomorphic structure in the grains after the first cycle. In addition, this graph shows that the first 3 rehydration cycles dehydrates at much higher temperatures than the last three. This is different from the measurements of $MgSO_4$ and proves us that by the rehydration at RH the crystals recrystallize to $CuSO_4.3H_2O$ and by an applied RH of 70%, the crystals are rehydrating to $CuSO_4.5H_2O$. This is in agreement with the values calculated from the signal intensities.

The rehydration process happens according to: firstly a fast rehydration to approximately $CuSO_4.3H_2O$ and secondly a slower rehydration process reaching the $CuSO_4.5H_2O$. No blocking was observed during the rehydration process as by $MgSO_4$.

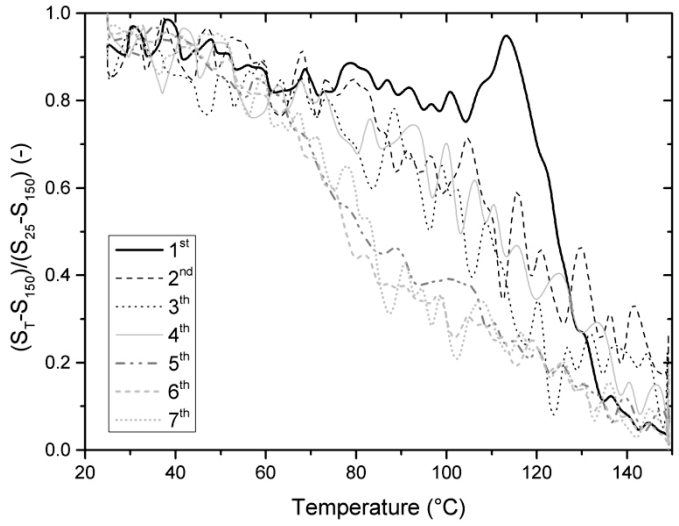

Figure 10: The water loss during the different dehydration runs scaled from 0-1 from the minimum (T = 150°C) till maximum (T = 25°C) water content in a single run. The first 4 runs are rehydrated at a RH of 50%, while the last three are rehydrated at a RH of 70%.

5. Conclusion

This study showed that the dehydration of salt hydrates with similar structures does not result in similar dehydration processes. The possibility of water release from the hydrated grains in combination with the solubility of the salt has a large influence on the dehydration process. Crystals can partially or completely dissolve, if the water cannot be released and vapor starts to condensate on the structure.

Two types of salts are selected for cyclic hydration/dehydration experiments: $CuSO_4$ and $MgSO_4$, because $MgSO_4$ partially dissolves and $CuSO_4$ shows no liquid water production. During cycling experiments we observe this dissolving only happens at the first dehydration run, if the crystals are dehydrating for the second time no liquid water is observed for the studied salt $MgSO_4$. In case of $CuSO_4$ no pore water was found during any cycles, but this salt shows also a difference between the first and other cycles. So in general the crystals cracks ones during dehydration, after this one time the crystals remain constant.

The largest difference between both rehydration cycles was the applied vapor pressure compared to the deliquescence RH. This can be the reason for the difference between $MgSO_4$ and $CuSO_4$ where in case of $MgSO_4$ the crystal shows different hydration/dehydration cycles each run and $CuSO_4$ did not.

From application point of view, the first dehydration cycle should be avoided, to avoid complete melting of the grain structure. In coming research we will focus on the rehydration, because our hypothesis is that during rehydration the vapor pathways are clogged. Experiments will be performed were the applied RH is raised above the deliquescence RH of $CuSO_4.H_2O$ to understand the observed difference between $MgSO_4$ and $CuSO_4$.

6. Acknowledgements

This research was carried out under the project number M75.7.11421 supported by TNO in the framework of

the Research Program of the Materials innovation institute (M2i) (www.m2i.nl).

7. References

P. M. A. Broers and G. S. A. van Welie, "The system CoSO4-H2O; vapour pressure measurements from 0° TO 150°C," *Recl. des Trav. Chim. des Pays-Bas*, vol. 84, no. 6, pp. 789–798, 1965.

P. M. A. Broers and G. S. A. van Welie, "Einiges uber das System CoSO4-H2O," *Zeitschrift fur Anorg. und Allg. Chemie*, vol. 346, pp. 221–224, 1966.

E. M. Crowther and J. R. H. Coutts, "A discontinuity in the Dehydration of Certain Salt Hydrates," *Proc. R. Soc. A*, vol. 106, no. 736, pp. 215–222, 1924.

Van Essen, V. M., Zondag, H. A., Gores, J. C., Bleijendaal, L. P. J., Bakker, M., Schuitema, R., Van Helden, W. G. J., 2009. Characterization of MgSO4 Hydrate for Thermochemical Seasonal Heat Storage. Journal of Solar Energy Engineering, 4, 134

Ervin, G., 1977, Solar heat storage using chemical reactions. Journal of Solid State Chemistry, 22 , 51–61.

Ford, R. W., and Frost, G. B., 1956, The low pressure dehydration of magnesium sulphate heptahydrate and cobaltous chloride hexahydrate," Canadian Journal of Chemistry, 591–599.

J. Hume and J. Colvin, "The Dehydration of Copper Sulphate Pentahydrate," *Proc. R. Soc. A Math. Phys. Eng. Sci.*, vol. 132, no. 820, pp. 548–560, Aug. 1931.

K. Kohler and P. Zaske, "Beitrage zur Therrnochemie der Hydrate. III, Der thermische Abbau van CoSO4.7H2O, FeSO4.7H2O, CuSO4.5H2O und die Isotypiebeziehungen der Abbauprodukte der Epsomit- und Melanteritreihe," *Z. anorg. allg. Chem.*, vol. 331, pp. 7–16, 1964.

Meiboom, S., Gill, D. 1958, Modified Spin-Echo Method for Measuring Nuclear Relaxation Times. Review of Scientific Instruments, 29, 688

J. C. Mutin and G. Watelle, "Study of a Lacunary Solid Phase and Kinetic Characteristics of its Formation," *J. Solid State Chem.*, vol. 28, pp. 1–12, 1979.

Pel, L., Kopinga, K., and Brocken, H., 1996, Determination of moisture profiles in porous building materials by NMR, Magnetic resonace imaging, 14, 931-932.

Y.-Q. Song, L. Venkataramanan, M. D. Hürlimann, M. Flaum, P. Frulla, and C. Straley, "T(1)--T(2) correlation spectra obtained using a fast two-dimensional Laplace inversion.," *J. Magn. Reson.*, vol. 154, no. 2, pp. 261–8, Feb. 2002.

M. Steiger, K. Linnow, D. Ehrhardt, and E. Rosenberg, "Decomposition reactions of magnesium sulfate hydrates and phase equilibria in the MgSO4–H2O and Na+–Mg2+–Cl−–SO42−–H2O systems with implications for Mars," *Geochim. Cosmochim. Acta*, vol. 75, no. 12, pp. 3600–3626, Jun. 2011.

E. W. Washburn, *International Critical Tables of Numerical Data, Physics, Chemistry and Technology (1st Electronic Edition)*, 2003.